

Application of incubation time approach to simulate dynamic crack propagation

V. Bratov · Y. Petrov

Received: 22 January 2007 / Accepted: 2 October 2007 / Published online: 19 October 2007
© Springer Science+Business Media B.V. 2007

Abstract The incubation time criterion for dynamic fracture is applied to simulate dynamic crack propagation. Being incorporated into ANSYS finite element package, this criterion is used to simulate the classical dynamic fracture experiments of Ravi-Chandar and Knauss on dynamic crack propagation in Homalite-100. In these experiments a plate with a cut simulating the crack was loaded by an intense pressure pulse applied on the faces of the cut. The load consisted of two consequent trapezoidal pulses. This, in the experimental conditions used by Ravi-Chandar and Knauss, resulted in a crack initiation, propagation, arrest and reinitiation. Dependence of the crack length on time was measured in those experiments. The results for crack propagation obtained by FEM modelling are in agreement with experimental measurements of crack length histories. This result shows the applicability of the incubation time approach to describe the initiation, propagation and arrest of dynamically loaded cracks.

Keywords Dynamic fracture · Incubation time · Crack initiation · Propagation · Arrest · FEM

1 Introduction

Studies in dynamic fracture date back to the first half of the 20th century when the first experimental results on fracture, caused by intensively applied loads (Hopkinson 1901; Wallner 1938; Schardin and Struth 1939; Wells and Post 1958) and the first analytical solutions for cracks moving with speeds comparable to that of a Reyleigh wave (Yoffe 1951; Broberg 1960; Atkinson and Eshelby 1968) appeared. Later, in the 1970's and early 1980's dynamics of fracture became a special area of interest for experimentalists and it was then that the main effects characterizing fracture under high loading rates were experimentally observed (Bradley and Kobayashi 1970; Kobayashi et al. 1974; Dally 1979; Ravi-Chandar and Knauss 1984a, b, c, d; Dally and Shukla 1980; Kalthoff 1986, Dally and Barker 1988; Rosakis and Zehnder 1985). Along with this, the majority of analytical solutions, of dynamic fracture problems were published (Freund 1972a,b,c; Kostrov 1966; Kostrov and Nikitin 1970; Achenbach 1974; Willis 1975; Freund 1990; Broberg 1989). The 80's and early 90's were the time when modern approaches to fracture dynamics were formed.

Nowadays two main approaches to the description of dynamic crack initiation exist. The first one, originating from the works of Freund (1972a, b, c) and later

V. Bratov (✉) · Y. Petrov
Institute of Problems of Mechanical Engineering RAS,
199178 St.-Petersburg, Russia
e-mail: vladimir@bratov.com

Y. Petrov
St.-Petersburg State University, 198504 St.-Petersburg,
Russia
e-mail: yp@yp1004.spb.edu

developed by Rosakis, is based on an assumption that fracture criterion can be expressed as a function of the stress intensity factor rate: $K^d(t) < K_C^d(\dot{K}(t))$, with K^d being the dynamic stress intensity factor, changing in time, K_C^d being its critical value and dot denoting time derivative.

This approach is able to describe some of the experimentally observed phenomena of dynamic fracture, mainly in the case of well-developed plasticity (though still within the framework of small scale yielding). The limitation of this approach is that, as shown in multiple works (ex. Owen et al. 1998), K_C^d used in the proposed criterion not only depends on loading rate and fractured material properties, but is also a function of experimental geometry and loading conditions. This means that experimentally measured K_C^d cannot be treated as a material property and cannot be used directly to model experiments with other geometries and loading conditions.

2 Incubation time criterion

Another approach that is able to describe crack initiation in dynamic conditions was formulated in Petrov and Morozov (1994) and Morozov and Petrov (2000). This criterion for fracture at a point x , at time t , reads as:

$$\frac{1}{\tau} \int_{t-\tau}^t \frac{1}{d} \int_{x-d}^x \sigma(x^*, t^*) dx^* dt^* \geq \sigma_c, \quad (1)$$

where τ is the microstructural time of a fracture process (or fracture incubation time)—a parameter characterizing the response of the material to applied dynamical loads (i.e. τ is constant for a given material and does not depend on problem geometry, the way a load is applied, the shape of a load pulse or its amplitude). d is the characteristic size of a fracture process zone and is constant for the given material and chosen scale. σ is normal stress at a point, changing with time, and σ_c is its critical value (ultimate stress or critical tensile stress found in quasistatic conditions).

Assuming

$$d = \frac{2}{\pi} \frac{K_{IC}^2}{\sigma_c^2}, \quad (2)$$

where K_{IC} is a critical stress intensity factor for mode I loading (mode I fracture toughness), measured in quasistatic experimental conditions, it can be shown that within the framework of linear fracture mechanics, for

the case of fracture initiation in the tip of an existing crack, (1) is equivalent to:

$$\frac{1}{\tau} \int_{t-\tau}^t K_I(t^*) dt^* \geq K_{IC}. \quad (3)$$

Condition (2) arises from the requirement that (1) is equivalent to Irwin's criterion ($K_I \geq K_{IC}$), in the case of $t \rightarrow \infty$.

As it was shown in many previous publications, criterion (3) can be successfully used to predict fracture initiation for brittle solids (ex. Petrov et al. 2003, Petrov and Sitnikova 2005). For slow loading rates and, hence, times to fracture that are much bigger than τ , condition (3) for crack initiation gives same predictions as Irwin's criterion of a critical stress intensity factor. For high loading rates and times to fracture comparable with τ all the variety of effects experimentally observed in dynamic experiments (ex. Ravi-Chandar and Knauss 1984a; Kalthoff 1986; Dally and Barker 1988) can be obtained using (3), both qualitatively and quantitatively (Petrov 2004). Application of condition (3) to the description of real experiments or usage of (3) as the critical fracture condition in finite element numerical analysis gives a possibility of better understanding of the nature of fracture dynamics (ex. Bratov et al. 2004), and even predicts new effects typical for dynamic processes (ex. Bratov and Petrov 2007). There is also the possibility of describing other highly transient processes on the basis of the incubation time approach (Petrov 2004). Using this ideology one can successfully model effects typical for electrical breakdown in insulators under high-rate pulsed voltage, cavitation of liquids, plasticity and phase transformations under high rate loads, detonation, etc., that are difficult to describe within the framework of classical approaches.

The present investigation is the very first attempt to apply criterion (1) to describe dynamic crack propagation. The criterion (3), while able to predict dynamic crack initiation, cannot be used to describe crack development in dynamic conditions. The main reason for this is that time dependency of a stress intensity factor in the tip of a crack moving at high speeds does not directly reflect the history of stress–strain fields in the vicinity of a current crack tip location as discussed by Ma and Freund (1986) and Ravi-Chandar and Knauss (1987).

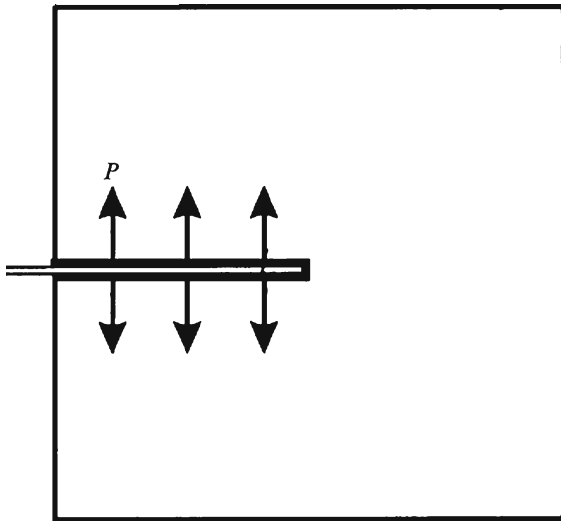


Fig. 1 Experimental scheme used by Ravi-Chandar and Knauss (1984a)

Though (3) is easier to use when simply describing crack initiation, (1) was used even to assess early stages of fracture development.

3 Classical experiments of Ravi-Chandar and Knauss

To check the ability of the criterion (1) to describe dynamic crack development, an attempt was made to simulate the classical fracture dynamics experiments reported by Ravi-Chandar and Knauss in 1984 (Ravi-Chandar and Knauss 1984a). In these experiments a rectangular sample with a cut simulating a crack is loaded by applying an intense load pulse to the crack faces. Figure 1 presents the experimental scheme and Fig. 2 gives an approximation of the load applied to the crack faces.

The behavior of the loaded sample is described by the Lamé equations:

$$\rho u_{i,tt} = (\lambda + \mu)u_{j,ji} + \mu u_{i,jj}, \tag{4}$$

where “,” refers to the partial derivative with respect to time and spatial coordinates. ρ is the mass density, and the indices i and j assume the values 1 and 2. Displacements are given by u_i in the directions x_i , respectively. t stands for time, λ and μ are Lamé constants. Stresses are coupled with strains by Hooke’s law:

$$\sigma_{ij} = \lambda \delta_{ij} u_{k,k} + \mu (u_{i,j} + u_{j,i}). \tag{5}$$

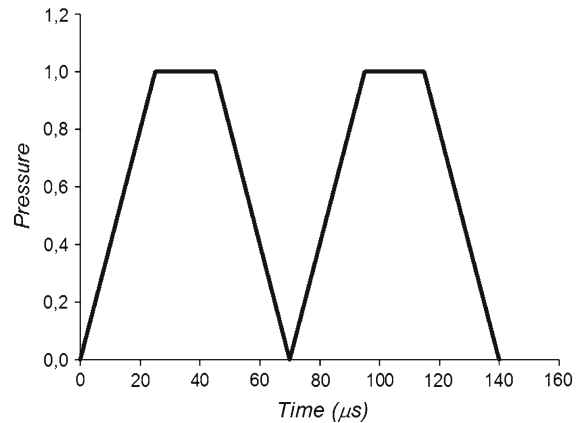


Fig. 2 Temporal shape of pressure pulse released in experiments by Ravi-Chandar and Knauss (1984a)

where σ_{ij} represents components of the stress tensor, δ_{ij} is the Kronecker delta assuming value of 1 for $i = j$ and 0 otherwise. At $t = 0$ the sample is stress free and velocity field is zero everywhere in the body:

$$\sigma_{ij}|_{t=0} = u_{,i}|_{t=0} = 0. \tag{6}$$

The crack faces are free from tractions:

$$\sigma_{21}|_{x_1 < 0, x_2 = 0} = 0. \tag{7}$$

The load applied to the crack faces is given by:

$$\sigma_{22}|_{x_1 < 0, x_2 = 0} = Af(t). \tag{8}$$

where $f(t)$ is given graphically in Fig. 2 and A is the amplitude of the load. The load was created by electromagnetic experimental equipment. The authors create an intense electric discharge that is passed through a flat conductor that is inserted into the crack. This electric discharge results in a repulsing force between the conductors. This creates a pressure pulse, constant over the cut surface and with a shape and amplitude controlled by the electric flow in the conductor, which can be easily measured.

Figure 3a and b present some of the results presented by Ravi-Chandar and Knauss. Figure 3a gives the stress intensity factor history for four of the experiments conducted. Figure 3b gives the crack propagation histories for the same experiments. Even though all of the experiments presented were conducted under nominally identical conditions, the results shown do differ. This can be explained by the slightly different charge accumulated in condensers prior to discharge through a conductor, resulting in a slightly different amplitude of electric flow and, hence, a different amplitude of pressure created on crack surfaces. Another possible reason for this

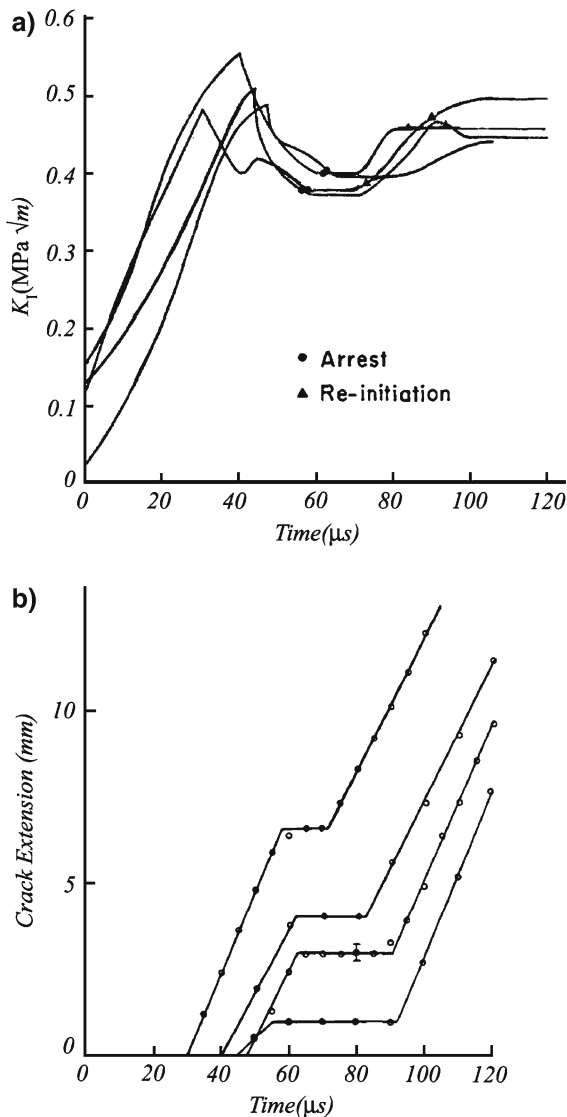


Fig. 3 (a) Stress intensity factor histories for crack arrest experiments (Ravi-Chandar and Knauss 1984a); (b) Crack extension histories for crack arrest experiments (Ravi-Chandar and Knauss 1984a)

difference that the authors mention is a slight disparity in sample geometry from experiment to experiment.

Unfortunately, in the article by Ravi-Chandar and Knauss (1984a) there is no information about the amplitude of pressure created in the presented experiments. Also, as it can be seen from Fig. 3b, at $t = 0$ the initial crack is already prestressed ($K_I(0) \neq 0$).

To check the ability of (1) to describe dynamic crack propagation the experimental conditions of Ravi-Chandar and Knauss (1984a) were modeled utilizing the finite element method.

4 Finite element formulation

In order to obtain a closed mathematical description of the dynamic fracture problem (4)–(8) is supplemented with fracture criterion (1). Due to symmetry, we suppose that the crack can propagate only along the x_1 axis. When condition (1) is fulfilled somewhere along a crack path, we suppose creation of a new surface in that point. Time integration in (1) is performed numerically using the trapezoidal rule.

The problem defined by (1) and (4)–(8) is solved numerically utilizing the finite element method. ANSYS finite element package was used to implement (4)–(8), and the fulfillment of condition (1) was checked by an external program after each time step (ANSYS User's Guide 2006).

Rectangular 4-node elements were used to mesh a body. The size of elements along the crack path was taken to be exactly $d = \frac{2}{\pi} \frac{K_{IC}^2}{\sigma_c^2}$. A reason for such a choice of element size is that d is a size that characterizes fracture on a chosen scale. From this point of view all the defects and spatial discontinuities with sizes essentially less than d cannot be called fractures within the framework of the scale used. Since critical stress intensity factors and ultimate stresses evaluated in laboratory conditions are used, then, by this, a scale to be used is set up. If, searching for K_{IC} and σ_c , one using experiments performed on, for example, geological or microscopic scales, one will get values for the studied fracture parameters, different from those acquired while testing specimens on a laboratory scale, and, hence one will get a different value for d , giving a characteristic size for the scale one is currently using.

Following this ideology, the size of an element used in the FE model along the crack path is the minimal size of a crack that we can call a “fracture”. Analogously, d is the minimal increment of a crack length that we can call “crack propagation” on a chosen scale. In the FE model used, release of a node along the crack path increases existing crack length by d —basic crack propagation takes place. Such a choice of an element size also simplifies spatial integration in (1).

Using the symmetry of the problem across the x_1 axis the problem was solved only for the upper half of the sample. Dimensions of the modeled sample were the same as in the experiments of Ravi-Chandar and Knauss (1984a). Figure 4a presents a mesh used in the solution. Fig. 4b gives details on the mesh surrounding

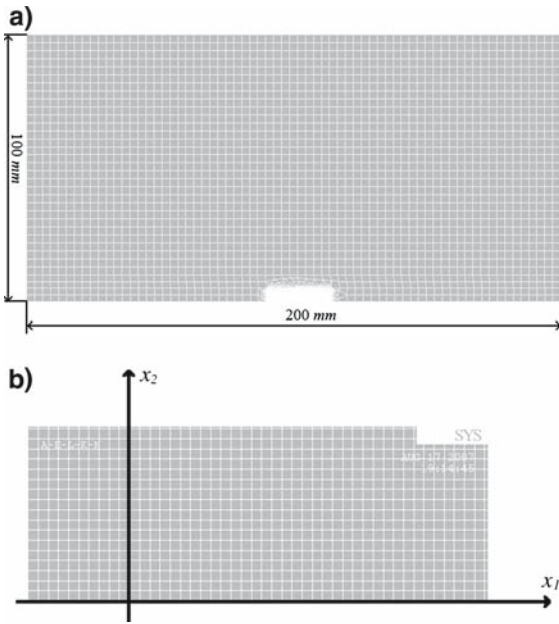


Fig. 4 (a) Mesh used in the FE model; (b) Mesh surrounding the crack tip

the crack tip. The crack can propagate along the x_1 axis within the zone with the fine mesh adjacent to the crack tip. The length of this zone is 17 mm.

A total of 18,621 nodes and 18,404 elements were used to form the mesh. Small elements with sizes equal to d are placed adjacent to the crack path to provide the needed accuracy of computation. Distant elements are larger in order to minimize the computational time and expense.

Due to the symmetry of the problem the crack path should follow the x_1 -axis. Nodes along the path are subjected to symmetrical boundary conditions up to the moment when the condition (1) is satisfied at a particular node (node movements in the vertical direction are restricted). At this moment the restriction on movement of the particular node is removed and a new surface is created. The technique used is similar to the node release technique.

The shape of the pressure pulse applied to the crack faces is given by Fig. 2, and its amplitude A is alternated in simulations. Material parameters typical for Homalite-100, used in the experiments of Ravi-Chandar and Knauss, were used in the calculations. These parameters are presented in Table 1.

The microstructural time of the fracture process, τ , for Homalite-100 was found by Petrov et al. (2003)

Table 1 Properties of Homalite-100 used in numerical simulations

Density, ρ , $\frac{\text{kg}}{\text{m}^3}$	1,230
Young's modulus, E , MPa	3,900
Poisson's ratio, ν	0.35
Critical stress intensity factor, K_{IC} , Mpa \sqrt{m}	0.48
Ultimate tensile stress, σ_c , MPa	48
Incubation time of fracture, τ , μs	9

from analysis of experiments by Ravi-Chandar and Knauss (1984a). The values of the critical stress intensity factor and the ultimate tensile stress gives a value for d . It appears to be 0.1 mm for Homalite-100 on a laboratory size scale.

The constructed model was checked for convergence. Usage of smaller time steps and smaller elements does not significantly affect the computational results. The ability of the FEM model to solve the stated dynamic problem was also checked by comparing computational results to the analytical solution for the stress intensity factor in the tip of a crack prior to crack initiation. The analytical solution for K_I temporal dependence in the studied problem is given, for example, in Petrov and Morozov (1994). The FEM computed K_I temporal dependence matches the analytical result with a maximum disparity of not more than 5%. The good matching between the computational and analytical result shows the applicability of the constructed model to the investigation of the problem stated by (4)–(8). Figure 5 gives a comparison between the experimental data of Ravi-Chandar and Knauss (1984a) for stress intensity factor at crack initiation for different times-to-fracture (i.e. different amplitudes of applied load pulse), and the analytical solution using criterion (3). The figure is reprinted from Petrov and Morozov (1994). This result shows that criterion (1), being the more general form of (3), has the ability to describe the crack initiation problem.

5 Results

After the stated problem is solved by the ANSYS FEM package, together with an external program controlling crack propagation, information about K_I time dependency and the crack extension history is provided for further analysis. $K_I(t)$ is computed using the asymptotic behavior of the stress field surrounding the crack tip.

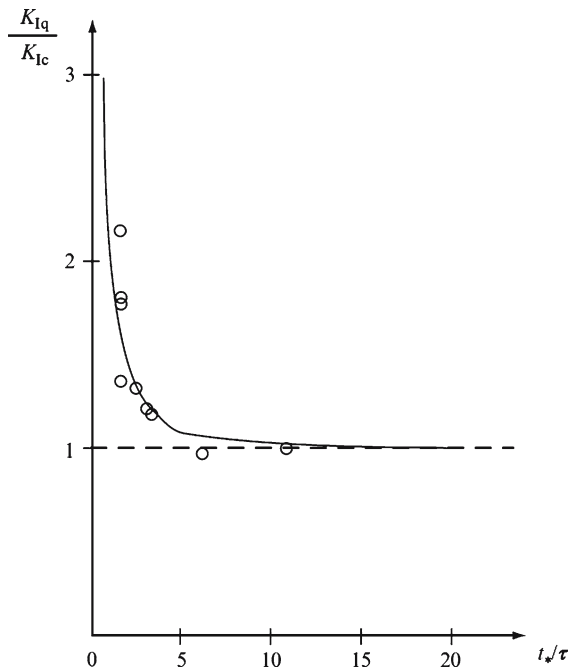


Fig. 5 Dependence of the normalized stress intensity factor at crack initiation on normalized time-to-fracture. Comparison of experimental data to analytical results obtained using crack initiation criterion (3)

It was observed that, depending on the amplitude of the applied pressure pulse A , three different modes of crack propagation are possible. The first one is trivial—amplitude that is too low results in no crack extension. The second one is the mode observed by Ravi-Chandar and Knauss (Fig. 3b). The crack starts propagating at a constant speed. Then it arrests, due to the energy flow into the crack tip which is no longer sufficient for its propagation. When the energy from the second trapezoid of the loading pulse approaches the crack tip region, the crack reinitiates and starts propagating at approximately the same speed as in the first stage of its extension (Fig. 6a).

Further increase of load amplitude A results in a propagation mode change. Now the crack is initiated, propagates at some constant speed, and when the energy from the second part of the loading pulse is delivered to the crack tip region the crack is accelerated and continues propagation at a higher speed (Fig. 6b).

By adjusting the pressure amplitude A , it was found that amplitudes around 5 MPa result in crack extension histories very close to those observed by Ravi-Chandar and Knauss (1984a). In Fig. 7, the computational result

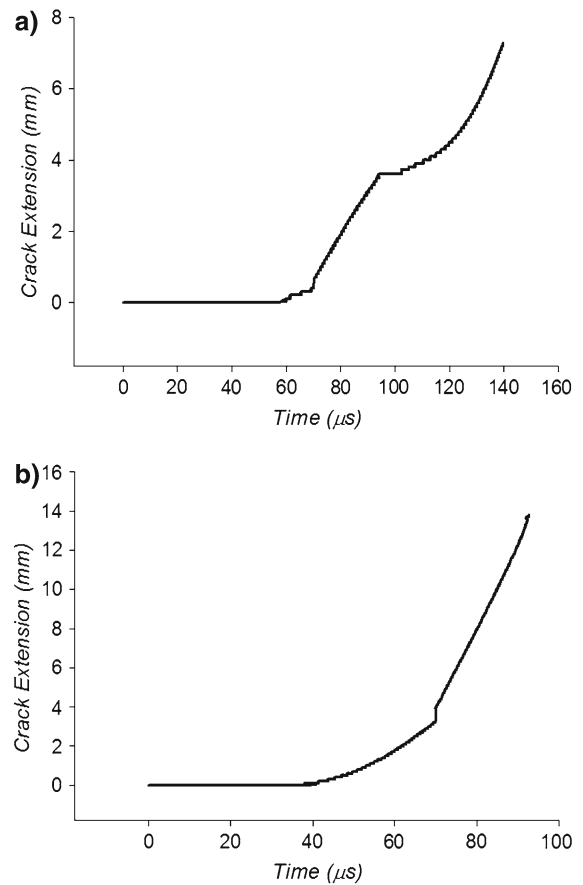


Fig. 6 (a) Crack extension history. $A = 5$ MPa; (b) Crack extension history. $A = 12$ MPa

for $A = 5.1$ MPa is compared to one of the experiments presented in Fig. 3b.

6 Conclusions

It has been shown that, solving the dynamic problem of linear elasticity by FEM and criterion (1) being used to assess critical conditions for crack advancement, the propagation of dynamically loaded cracks can be predicted. It has also been shown that criterion (1) with d , chosen from the condition of coincidence of (1) with Irwin's criterion in static conditions can be used to describe dynamic crack initiation, propagation and arrest.

Criterion (1), unlike (3), which is applicable only to crack initiation, can also be used as the condition for crack propagation and arrest. In the presented model

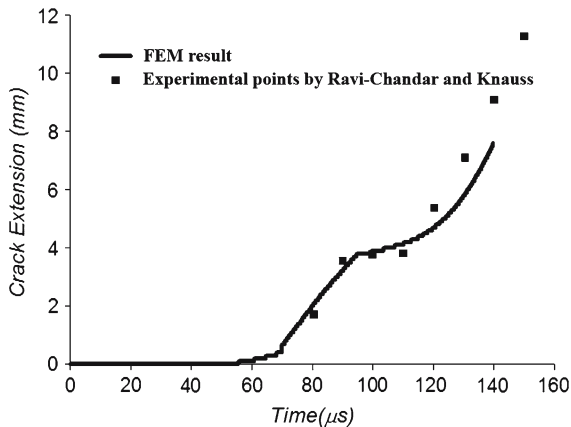


Fig. 7 Crack extension history. Comparison of FEM calculation with the experimental data points of Ravi-Chandar and Knauss (1984a)

(1) is used as a condition for node release. This criterion does not even require the presence of a crack. Thus, the condition for crack propagation and arrest appears automatically. The crack propagates whilst (1) is fulfilled for nodes ahead of the moving crack tip; otherwise the crack arrests.

Using a similar method one can model cracks that change their direction of propagation and even branch. In this case (1) should be applied not only to stresses acting perpendicular to the x_1 direction, as is done in the presented research, but in all the possible directions surrounding the x^* point.

According to the incubation-time based approach by Petrov and Morozov (see Petrov 1991, (in Russian) or Petrov and Morozov 1994), in combination with a variety of widely known experimental observations, the critical stress intensity factor at the crack initiation moment under high rate loads may, depending on the experimental geometry, loading conditions and history, either be noticeably smaller or greater than K_{IC} . This instability of dynamic fracture toughness is particularly evident while comparing two different load application histories (Petrov et al. 2003). In the first case, a suddenly applied dynamic load is maintained at a constant level up to the moment of crack initiation (ex. Smith 1975; Ravi-Chandar and Knauss 1984a; Rizal and Homma 2000; Homma et al. 1992). In this case K_I^d usually significantly exceeds the static K_{IC} . In the second case, when the fracture is excited by short load pulses with time shapes close to the delta function, threshold amplitude, K_I^d is usually significantly

less than K_{IC} (ex. Atroschenko et al. 2002; Shokey et al. 1986).

This reasoning shows that the dynamic fracture toughness, K_I^d , is not an intrinsic characteristic of a material and that usage of critical stress intensity factor criterion ($K_I(t) \geq K_I^d$) to describe dynamic fracture initiation cannot be universally correct. For the same reasons it is impossible to describe dynamic fracture initiation using rate dependent K_I^d . Application of the incubation-time based approach allows one to describe all variety of experimentally observed effects in fracture dynamics. An important consequence of this approach is that it provides an effective way of testing dynamic strength by direct measurement of τ , a parameter intrinsic to the material and not dependent on experimental geometry or the way the load is applied (Petrov 2004). This provides a tool that can be directly incorporated into practical engineering.

The results presented in the current paper show that a similar approach can be successfully used to describe dynamic crack propagation and arrest.

Remarkable progress in modern computational fracture dynamics is connected with the introduction of cohesive zone models into finite element and other numerical schemes. The idea that Barenblatt originally proposed as a model for quasistatic cracks (Barenblatt 1962) appeared to be very useful also for dynamic cracks (ex. Xu and Needleman 1995; Camacho and Ortiz 1996; Remmers et al. 2004). It was shown that incubation time fracture criterion can be reformulated into a kind of cohesive law (Morozov and Petrov 2000). This means it is possible to create a cohesive zone model providing results identical to the predictions made by the incubation time approach used in the current study.

References

- Achenbach JD (1974) Dynamic effects in brittle fracture. In: Nemat-Nasser S et al (eds) *Mechanics today*, 1. Pergamon, Elmsford, NY, pp 1–57
- ANSYS (2006) *User's Guide*, Release 11.0. ANSYS Inc., Pennsylvania, USA
- Atkinson C, Eshelby JD (1968) The flow of energy into the tip of a moving crack. *Int J Fract* 4:3–8
- Atroschenko SA, Krivosheev SI, Petrov YV (2002) Crack propagation upon dynamic failure of polymethylmethacrylate. *Tech Phys* 47:194–199
- Barenblatt GI (1962) The mathematical theory of equilibrium cracks in brittle fracture. *Adv Appl Mech* 7:55–129

- Bradley WB, Kobayashi AS (1970) An investigation of propagating crack by dynamic photoelasticity. *Exp Mech* 10:106–113
- Bratov V, Gruzdkov A, Krivosheev S, Petrov Y (2004) Energy balance in the crack growth initiation under pulsed-load conditions. *Doklady Phys* 49:338–341
- Bratov V, Petrov Y (2007) Optimizing energy input for fracture by analysis of the energy required to initiate dynamic mode I crack growth. *Int J Solid Struct* 44:2371–2380
- Broberg KB (1960) The propagation of a brittle crack. *Archiv fur Fysik* 18:159–192
- Broberg KB (1989) The near-tip field at high crack velocities. *Int J Fract* 39:1–13
- Camacho GT, Ortiz M (1996) Computational modelling of impact damage in brittle materials. *Int J Solid Struct* 33:2899–2938
- Dally JW (1979) Dynamic photoelastic studies of fracture. *Exp Mech* 19:349–361
- Dally JW, Shukla A (1980) Energy loss in Homalite-100 during crack propagation and arrest. *Eng Fract Mech* 13:807–817
- Dally JW, Barker DB (1988) Dynamic measurements of initiation toughness at high loading rate. *Exp Mech* 28:298–303
- Freund LB (1972a) Crack propagation in an elastic solid subjected to general loading. I: Constant rate of extension. *J Mech Phys Solid* 20:129–140
- Freund LB (1972b) Crack propagation in an elastic solid subjected to general loading. II: Nonuniform rate of extension. *J Mech Phys Solid* 20:141–152
- Freund LB (1972c) Energy flux into the tip of an extending crack in an elastic solid. *J Elast* 2:341–349
- Freund LB (1990) *Dynamic fracture mechanics*. Cambridge University Press, Cambridge
- Homma H, Kanto Y, Tanka K (1992) Rapid load fracture testing. In: Chona R, Corwin WR (eds) *Cleavage fracture under short stress pulse loading at low temperatures*, ASTM STP 1130. American society for testing and materials, Philadelphia, pp 37–49
- Hopkinson J (1901) *Original Papers*. Cambridge University Press
- Kalthoff JF (1986) Fracture behavior under high rates of loading. *Eng Fract Mech* 23:289–298
- Kobayashi AS, Wade BG, Bradley WB, Chiu ST (1974) Crack branching in Homalite-100 plates. *Eng Fract Mech* 6:81–92
- Kostrov BV (1966) Unsteady propagation of longitudinal shear cracks. *Appl Math Mech* 30:1241–1248
- Kostrov BV, Nikitin LV (1970) Some general problems of mechanics of brittle fracture. *Archiwum Mechaniki Stosowanej* 22:749–775
- Ma CC, Freund LB (1986) The extent of the stress intensity factor field during crack growth under dynamic loading conditions. *ASME J Appl Mech* 53:303–310
- Morozov N, Petrov Y (2000) *Dynamics of fracture*. Springer-Verlag, Berlin
- Owen DM, Zhuang S, Rosakis AJ, Ravichandran G (1998) Experimental determination of dynamic crack initiation and propagation fracture toughness in aluminum sheets. *Int J Fract* 90:153–174
- Petrov YV (1991) On “Quantum” Nature of Dynamic Fracture of Brittle Solids. *Doklady Akademii Nauk USSR* 321:66–68
- Petrov YV, Morozov NF (1994) On the modeling of fracture of brittle solids. *J Appl Mech* 61:710–712
- Petrov YV, Morozov NF, Smirnov VI (2003) Structural micromechanics approach in dynamics of fracture. *Fatig Fract Eng Mater Struct* 26:363–372
- Petrov YV (2004) Incubation time criterion and the pulsed strength of continua: fracture, cavitation, and electrical breakdown. *Doklady Phys* 49:246–249
- Petrov Y, Sitnikova E (2005) Temperature dependence of spall strength and the effect of anomalous melting temperatures in shock-wave loading. *Tech Phys* 50:1034–1037
- Ravi-Chandar K, Knauss WG (1984a) An experimental investigation into dynamic fracture: I. Crack initiation and arrest. *Int J Fract* 25:247–262
- Ravi-Chandar K, Knauss WG (1984b) An experimental investigation into dynamic fracture: II. Microstructural aspects. *Int J Fract* 26:65–80
- Ravi-Chandar K, Knauss WG (1984c) An experimental investigation into dynamic fracture: III. On steady state crack propagation and crack branching. *Int J Fract* 26:141–154
- Ravi-Chandar K, Knauss WG (1984d) An experimental investigation into dynamic fracture: IV. On the interaction of stress waves with propagating cracks. *Int J Fract* 26:189–200
- Ravi-Chandar K, Knauss WG (1987) On the characterization of the transient stress field near the tip of a crack. *J Appl Mech* 54:72–78
- Remmers JJC, Borst R de, Needleman A (2004) A cohesive segments approach for dynamic crack growth. In: Ahzi S, Cherkaoui M, Khaleel MA, Zbib HM, Zikry MA, Lamatina B (eds) *Multiscale modeling and characterization of elastic-inelastic behavior of engineering materials*. Kluwer, Dordrecht, pp 299–306
- Rizal S, Homma H (2000) Dimple fracture under short pulse loading. *Int J Impact Eng* 90:83–102
- Rosakis AJ, Zehnder AT (1985) On dynamic fracture of structural metals. *Int J Fract* 27:169–186
- Schardin H, Struth W (1938) Hochfrequenzkinematographische untersuchung der bruchvorgänge in glas. *Glastechnische Berichte* 16:219
- Shokey DA et al (1986) Short pulse fracture mechanics. *J Eng Fract Mech* 23:311–319
- Smith GC (1975) An experimental investigation of the fracture of a brittle material, Ph.D. Thesis, California Institute of Technology
- Wallner H (1938) Linienstrukturen an bruchflächen. *Z. Physik* 114:368–370
- Wells AA, Post D (1958) The dynamic stress distribution surrounding a running crack—A photoelastic analysis. *Proc Soc Exp Stress Anal* 16:69–93
- Willis JR (1975) Equations of motion for propagating crack. *Mech Phys Frac, The Metals Soc, London* 1:57–67
- Xu X, Needleman A (1995) Numerical simulations of dynamic crack growth along an interface. *Int J Fract* 74:289–324
- Yoffe EH (1951) The moving Griffith crack. *Phil Mag* 42:739–750